22nd International Conference on Sustainable Energy Technologies
Kuala Lumpur, Malaysia, 13 to 15 August 2026 · ISBN 978-1-995850-00-9 · ISSN 2978-4387

CONFERENCE PAPER · ENERGY STORAGE & CONVERSION

Coupled Effects of Thermodynamic Conditions, Bed Configuration and Airflow Characteristics on the Performance of an Open-Loop Thermochemical Energy Storage Reactor

Zhuo Chang[1]*, Eleonora Baccega[1], Moussa Aidi[1], Michele Bottarelli[1]

[1] Department of Architecture, University of Ferrara, Ferrara, Italy

RECEIVED 5 May 2026 · REVISED 2 June 2026 · ACCEPTED 13 June 2026
PRESENTED 13 to 15 August 2026 · PUBLISHED 23 November 2026

ABSTRACT

Open-loop thermochemical energy storage (TCES) can support low-temperature heat storage, but reactor performance depends on the interaction between adsorption conditions and transport through the packed bed. This study examined the effect of elevated inlet temperature and reinterpreted the discharge behaviour of a laboratory-scale COCO reactor filled with a $CaCl_2$-vermiculite composite. The analysis considered inlet temperature, absolute humidity, airflow velocity and bed thickness. A series of 1 h adsorption tests was evaluated using the outlet-to-inlet temperature difference, average specific power, cumulative specific energy and change in state of charge. The water-vapour pressure ratio described the thermodynamic adsorption conditions, while the characteristic residence time (τ), derived from bed thickness and superficial air velocity, represented transport conditions. The experiments covered bed thicknesses of 5, 10 and 15 cm, airflow velocities of 0.2 and 0.4 $m \cdot s^{-1}$, inlet absolute humidities of about 6 and 12 $g_w \cdot kg_{da}^{-1}$, and inlet temperatures of about 18 and 43–50 °C. Increasing the inlet temperature reduced the pressure ratio (r_p) from about 3.02–6.47 to 0.87–2.51 and limited cumulative specific energy to approximately 60–70 $Wh \cdot kg^{-1}$. Thicker beds maintained a higher temperature rise, but the 5 cm bed achieved the highest specific energy per unit mass under low-temperature conditions, indicating lower material utilisation in thicker beds. At comparable characteristic residence times, increasing inlet humidity from about 6 to 12 $g_w \cdot kg_{da}^{-1}$ produced up to a twofold increase in average specific power. Higher airflow increased vapour delivery and heat extraction despite reducing nominal residence time. The findings showed that pressure ratio and characteristic residence time provided complementary descriptions of reactor behaviour. A preliminary empirical correlation was developed, and the initial fitting indicated that inlet temperature and airflow velocity had the largest effects on peak power and discharge-curve shape. These results provided a practical basis for selecting operating conditions and bed configurations in building-scale open-loop TCES systems.

KEYWORDS Thermochemical energy storage, Vermiculite-$CaCl_2$ composite, Pressure ratio, Characteristic residence time

1. Introduction

The increasing use of renewable energy has increased the need for thermal storage technologies that can balance variations between energy supply and demand (Suraparaju *et al.* 2025). Thermochemical energy storage (TCES) stores heat through reversible sorption reactions and can provide a higher energy storage density with lower long-term storage losses than sensible and latent heat storage (Enasel and Dumitrascu 2025). The performance of these reversible reactions depends on thermochemical materials that can repeatedly adsorb and desorb water vapour under different operating conditions. The sorption material determines how much water vapour can be adsorbed

* Corresponding author. Email address: chnzhu@unife.it (Zhuo Chang)

© 2026 The Author(s).
Published by Caravel Press.

doi.org/10.65582/set.2026.009

and how much heat can be released. The reactor, however, determines whether this storage potential can be used under practical conditions. Material selection and reactor design must therefore be considered together, particularly in open TCES systems, where humid air drives the reaction and transfers the released heat through the material bed (Zeng *et al.* 2024; Kinzer *et al.* 2025).

Among hygroscopic salts, calcium chloride ($CaCl_2$) is commonly used in low-temperature TCES because of its low cost and high affinity for water vapour (Gaeini *et al.* 2018). However, pure $CaCl_2$ may deliquesce during hydration, which can lead to salt migration, agglomeration and poor mass transfer (Chen *et al.* 2025). Porous supporting materials have therefore been used to retain the salt and maintain the structure of the reactive bed. Expanded vermiculite is suitable for this purpose because its layered porous structure can accommodate $CaCl_2$ and form a stable granular composite (Aristov *et al.* 2000; Zhang *et al.* 2024). Recent studies on vermiculite-$CaCl_2$ composites have mainly examined how preparation methods and salt loading affect pore structure, storage capacity and hydration behaviour (Zhang *et al.* 2024; Chen *et al.* 2026). Other work has assessed the cycling stability of calcium-impregnated vermiculite during repeated charging and discharging processes (Sullivan *et al.* 2023). These studies described the storage potential and reaction behaviour of the composite. However, material-scale measurements did not fully represent its performance after it was placed in a packed-bed reactor.

At reactor scale, heat release also depended on water-vapour delivery, airflow distribution and transport through the material bed. Aydin *et al.* (2016) examined the effect of inlet humidity in an open vermiculite-$CaCl_2$ reactor. Hosouli *et al.* (2026) later showed that bed depth and moist-air flow rate changed the temperature rise and effective use of the storage material. Pressure losses caused by airflow through adsorption beds were also examined by Baghapour *et al.* (2018). However, the combined effects of inlet temperature, humidity, airflow velocity and bed thickness remained less clear. Reliable models were needed to link material-scale behaviour with practical reactor design. Detailed numerical models represented the coupled transport of heat, air and water vapour through porous beds. The simulations revealed performance limits associated with non-uniform flow, reaction kinetics and local temperature gradients (Gaeini *et al.* 2017; Baccega *et al.* 2025; Kieskamp *et al.* 2024). These models provided detailed results, but they required many input parameters and more computation than reduced-order methods. Gao *et al.* (2025) used a reaction-wave model to relate reactor output to design and operating variables. Valverde *et al.* (2024) also found that particle size affected adsorption kinetics and the movement of the adsorption front in a packed column. A model for engineering design therefore had to remain simple, include the main physical processes and be tested against reactor data.

Based on the research gaps identified above, these findings highlighted a common limitation: inlet temperature, humidity, airflow velocity and bed thickness were often interpreted separately, making it difficult to distinguish thermodynamic effects from transport-related limitations. To address this issue, we reanalysed the experimental data obtained from the laboratory-scale reactor, hereafter named COCO, under different operating conditions. The analysis focused on three linked aspects: the effect of temperature and humidity on adsorption conditions, the influence of airflow velocity and bed thickness on water-vapour delivery and material utilisation, and the possibility of interpreting these effects within a common physical framework. The tests were therefore reorganised using the water-vapour pressure ratio and characteristic residence time (τ) as thermodynamic and transport-related descriptors, respectively.

In this article, the thermodynamic state of the reactive bed was linked with the transport conditions inside the reactor. The pressure ratio (r_p) represented the combined effect of water-vapour availability and temperature on the adsorption conditions. It also reflected changes caused by bed thickness, since the amount of material and the bed temperature affected the equilibrium vapour pressure. The τ combined bed thickness with airflow velocity and was used to describe differences in air–material contact conditions. These two descriptors were not treated as independent predictors. Instead, they provided a common basis for comparing temperature rise, specific power, energy

release and material hydration under different test conditions. The theoretical contribution of this article lay in interpreting reactor performance through the joint effects of thermodynamic conditions and transport processes, rather than through separate operating parameters. The results also provided practical guidance for selecting bed thickness and airflow conditions under different inlet temperature and humidity levels in building heating applications.

2. Experimental methodology

2.1. Experimental facility

The experimental investigation was carried out using a laboratory-scale open-loop TCES system to evaluate the adsorption performance of the vermiculite-$CaCl_2$ composite under controlled operating conditions. We used the experimental setup shown in Figure 1. The system consisted of an air supply unit, a humidifier, an adsorption reactor, a power supply, a data acquisition system and a weighing system. Before each test, ambient air was humidified and then supplied to the reactor at the selected airflow and humidity conditions.

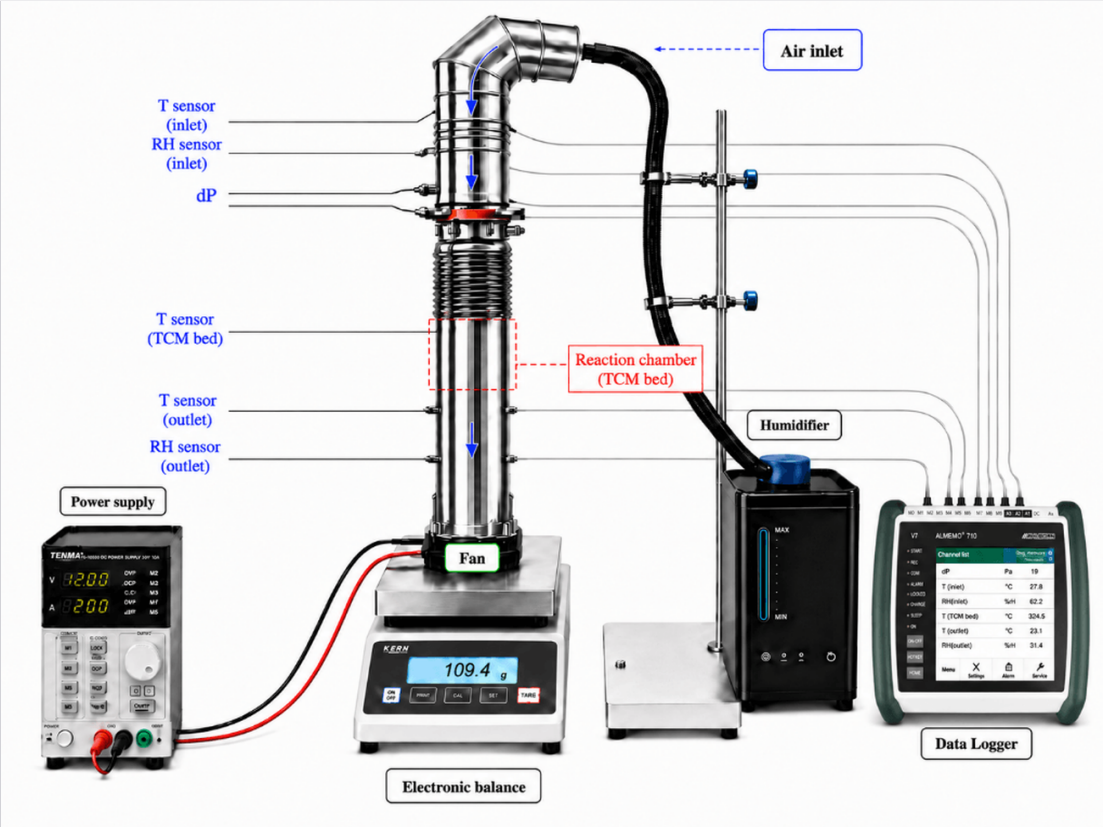

Figure 1. Laboratory-scale open-loop TCES experimental setup and sensor arrangement.

The adsorption reactor contained a modular packed-bed section with a maximum available bed height of 20 cm. This design allowed different bed thicknesses and material quantities to be tested without changing the main reactor geometry. A centrifugal fan generated the airflow through the reactor, while an ultrasonic humidifier (RAM, 13 L, Italy) supplied water vapour to the inlet air. The fan was powered by a programmable DC power supply (TENMA 72-2925, Tenma, UK). During the tests, the current was kept at 2.7 A, while the voltage was adjusted up to 12 V to obtain the required airflow condition.

Temperatures, relative humidities and differential pressure were recorded throughout each 1 h adsorption test using an ALMEMO® 710 multi-channel data logger (AHLBORN Mess- und Regelungstechnik GmbH, Germany). These measurements were used to assess the transient thermal

response of the reactor and to calculate the performance indicators analysed in this work. At the same time, the mass change of the TCM was measured using a FES 33K-4 laboratory precision balance (KERN & SOHN GmbH, Germany). The mass measurements were then used to determine the water uptake and the corresponding change in state of charge (ΔSoC).

The experimental setup maintained stable operating conditions and produced repeatable measurements across the investigated cases. The resulting dataset was used to analyse how thermodynamic conditions and transport processes affected the discharge performance of the open-loop TCES reactor.

2.2. Experimental dataset and comparison strategy

The experimental dataset was reorganised using two descriptors: τ and r_p. The τ represented the transport and air–material contact conditions, while r_p described the thermodynamic conditions of adsorption. These parameters were introduced to enable comparison among experiments conducted with different bed thicknesses, airflow velocities and inlet-air temperatures.

2.2.1. Characteristic residence time

The characteristic residence time, τ, was used as a simplified indicator of the time available for interaction between the humid airflow and the thermochemical material bed. It was calculated from the bed thickness and the superficial airflow velocity using Equation (1):

$$\tau = \frac{L_{bed}}{u} \tag{1}$$

Where:

- L_{bed} is the thickness of the TCM bed in the airflow direction (m)
- u is the air velocity through the reactor (m·s^{-1}).

According to Equation (1), increasing the bed thickness increases τ, whereas increasing the airflow velocity reduces it. However, τ should not be interpreted as an independently controlled parameter. A change in airflow velocity simultaneously modifies the air mass flow rate, water vapour supply rate and convective heat and mass transfer. Therefore, τ was employed in this study as a transport related descriptor rather than as the actual residence time distribution of the reactor. This interpretation is consistent with reactor design approaches in which mean residence time is related to reactor length and flow velocity, while the resulting conversion remains governed by the competition between reaction and transport processes.

2.2.2. Change in state of charge

The change in state of charge, ΔSoC, was used to quantify the fraction of the theoretical hydration capacity used during each adsorption test. It was calculated using Equation (2):

$$\Delta SoC = \frac{m_{final} - m_{initial}}{m_{TCM,0} \cdot x_{salt} \cdot w_{\max}} \tag{2}$$

Where:

- $m_{final} - m_{initial}$ = water uptake measured during the adsorption test (g);
- $m_{TCM,0}$ = initial mass of the TCM at the beginning of the test (g);

- x_{salt} = mass fraction of $CaCl_2$ in the composite, taken as 0.60;
- w_{max} = theoretical maximum water uptake ratio of $CaCl_2$, taken as 0.97 $g_w \cdot g_{CaCl_2}^{-1}$, corresponding to complete hydration from anhydrous $CaCl_2$ to $CaCl_2 \cdot 6H_2O$.

Equation (2) normalised the measured water uptake by the theoretical maximum hydration capacity of the $CaCl_2$ contained in the composite. A higher ΔSoC therefore indicated that a larger fraction of this capacity was used during the fixed 1 h adsorption period.

2.2.3. Water vapour pressure and pressure ratio

In the open-loop TCES reactor, water vapour carried by the airflow acted as the reactive gas. The saturation vapour pressure at the measured inlet-air temperature was first calculated using Equation (3):

$$p_{sat,in} = 0.611 \times \exp\left(\frac{17.27 \cdot T_{in}}{T_{in} + 273.15}\right) \tag{3}$$

The inlet water-vapour partial pressure was then obtained from the measured relative humidity using Equation (4):

$$p_v = p_{sat,in} \times \frac{RH_{in}}{100} \tag{4}$$

Where:

- $p_{sat,\,in}$ = saturation vapour pressure at the inlet air temperature (kPa)
- p_v = water vapour partial pressure (kPa)
- T_{in} = measured inlet air temperature (°C)
- RH_{in} = measured inlet relative humidity (%).

The equilibrium vapour pressure of the $CaCl_2$-based composite depended on the measured material temperature. It was calculated using the Van't Hoff relationship given in Equation (5):

$$\ln\left(\frac{p_{eq}}{p_0}\right) = -\frac{\Delta H_r}{R T_{TCM}} + \frac{\Delta S_r}{R} \tag{5}$$

The $CaCl_2 \cdot H_2O$/$CaCl_2 \cdot 2H_2O$ equilibrium curve was selected as a common reference for all tests. After drying at 130 °C, the TCM was considered nearly anhydrous and was expected to hydrate largely to the monohydrate state during cooling and exposure to ambient air. The higher hydration stages were not suitable as a common reference across all operating conditions. The 1↔2 transition was therefore used to compare the low- and high-temperature tests within a consistent thermodynamic framework. This choice did not imply that the material remained only within this hydration stage during adsorption.

Where:

- p_{eq} = equilibrium vapour pressure (kPa)
- p_0 = reference pressure (kPa)
- ΔH_r = reaction enthalpy for the transition from $CaCl_2 \cdot H_2O$ to $CaCl_2 \cdot 2H_2O$, 50.6 $kJ \cdot mol^{-1}$
- ΔS_r = reaction entropy for the transition from $CaCl_2 \cdot H_2O$ to $CaCl_2 \cdot 2H_2O$, 114 $J \cdot mol^{-1} \cdot K^{-1}$
- R = universal gas constant, 8.314 $J \cdot mol^{-1} \cdot K^{-1}$
- T_{TCM} = material temperature (K).

Using the inlet water-vapour partial pressure from Equation (4) and the equilibrium vapour pressure from Equation (5), the pressure ratio was calculated using Equation (6):

$$r_p = \frac{p_v}{p_{eq}} \tag{6}$$

Equation (6) compared the actual water-vapour pressure with the equilibrium pressure of the 1↔2 hydration transition. A value above unity indicated that hydration towards $CaCl_2 \cdot 2H_2O$ was thermodynamically favoured, while a value below unity indicated that the operating condition was below this equilibrium boundary. The pressure ratio was used as a thermodynamic descriptor rather than as a direct measure of the actual hydration state.

2.2.4. Investigated parameters and operating ranges

The experimental programme considered different bed thicknesses, airflow velocities, inlet absolute humidities and inlet temperatures. The selected parameter ranges and their intended roles in the present analysis are summarised in Table 1.

Table 1. Experimental variables investigated ranges and their roles in the present analysis.

Parameter	Levels	Purpose
Bed thickness	5/10/15 cm	transport limitation
Air velocity	0.2/0.4 $m \cdot s^{-1}$	Air and water vapour supply, convective transport
Absolute humidity	6/12 $g_w \cdot kg_{da}^{-1}$	Water vapour availability and adsorption potential
Inlet temperature	~18 °C / 43–50 °C	Material thermal condition, equilibrium vapour pressure and thermodynamic adsorption behaviour

The tests were subsequently reorganised into three comparison groups. The first group examined the transient influence of inlet temperature and bed thickness. The second analysed the relationships between pressure ratio and the measured performance indicators. The third investigated the coupled effects of τ and inlet absolute humidity. This grouping enabled the same experimental database to be interpreted from thermodynamic and transport related perspectives rather than as a series of isolated operating cases.

3. Results and Discussion

3.1. Effect of inlet temperature and bed thickness on transient thermal performance

Since inlet temperature altered the adsorption equilibrium and bed thickness changed both the amount of reactive material and the internal transport path, their combined influence on reactor performance was examined. Tests conducted at approximately 18–19 °C and 43–50 °C were compared across three TCM bed thicknesses. The outlet to inlet temperature difference was used to characterise the transient thermal response, while cumulative specific energy quantified the energy released per unit mass of TCM. Figure 2 presents the evolution of both indicators during the 60 min adsorption tests.

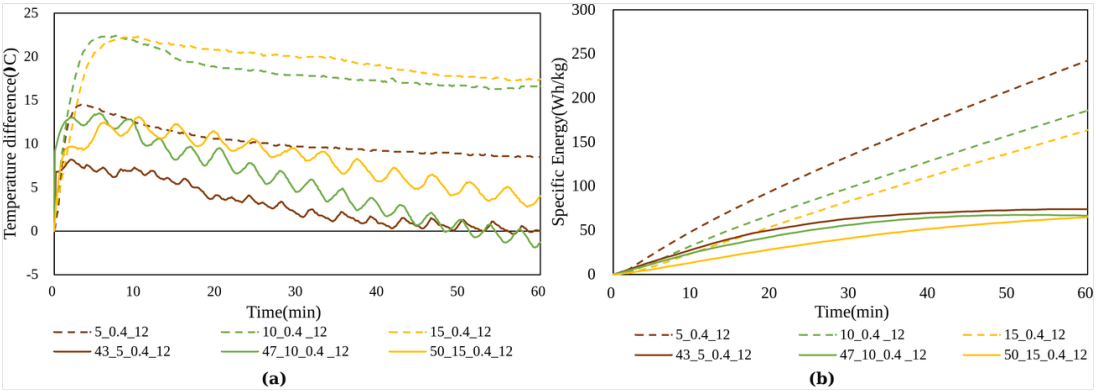

Figure 2. Effect of inlet temperature and TCM bed thickness on the transient thermal performance of the COCO reactor: (a) temperature difference between the reactor outlet and inlet; and (b) cumulative specific energy output.

The reactor showed different thermal responses at the two inlet temperature levels. At low inlet temperatures (~18 °C), the ΔT peaks rapidly during the initial adsorption phase before gradually declining, maintaining positive values throughout the 60-minute cycle. Increasing the TCM bed thickness yields a higher and more sustained ΔT, with the 10 cm and 15 cm configurations consistently outperforming the 5 cm bed. Conversely, at elevated inlet temperatures (~43–50 °C), the initial thermal response was lower and decays rapidly, occasionally yielding slightly negative ΔT values toward the end of the test. Rather than definitively indicating desorption, this negative differential likely stems from reactor heat losses, thermal inertia, or transient temperature gradients between the inlet air and the bed matrix. Nevertheless, the beneficial effect of a greater amount of reactive material remains observable across both regimes, though its magnitude is severely attenuated at higher temperatures.

This temperature dependent divergence is further reflected in the cumulative specific energy curves. At low inlet temperatures, specific energy increases continuously. Crucially, despite generating lower temperature lifts, the 5 cm configuration achieves the highest specific energy output, followed by the 10 cm and 15 cm beds. This indicates that increasing the reactive mass does not yield a proportional gain in useful energy, a limitation attributed to lower effective material utilization caused by extended internal transport paths and elevated heat and mass transfer resistances within thicker beds. Under high temperature conditions, the specific energy curves converge toward a narrow range (~60–70 Wh·kg^{-1}) regardless of bed thickness, with accumulation rates flattening significantly after 40–50 minutes. This result indicated that adding more material provided little additional benefit under restricted thermodynamic conditions.

Ultimately, these findings indicate that inlet temperature acts as more than a simple boundary condition; it directly dictates the reactive bed temperature and alters the underlying sorption equilibrium. However, because inlet temperature alone cannot fully define the thermodynamic state, the following section introduces r_p to evaluate whether these operational variances correlate directly with the material's adsorption potential.

3.2. Relationship between pressure ratio, bed thickness and reactor performance

To determine whether the different responses observed under low- and high-temperature conditions could be explained by the thermodynamic state of the reactive bed, r_p was compared with three performance indicators. The average temperature difference represented the thermal response, the average specific power described the rate of heat release, and ΔSoC indicated the extent of material hydration. Figure 3 presents these relationships for the different bed thicknesses and inlet temperature conditions.

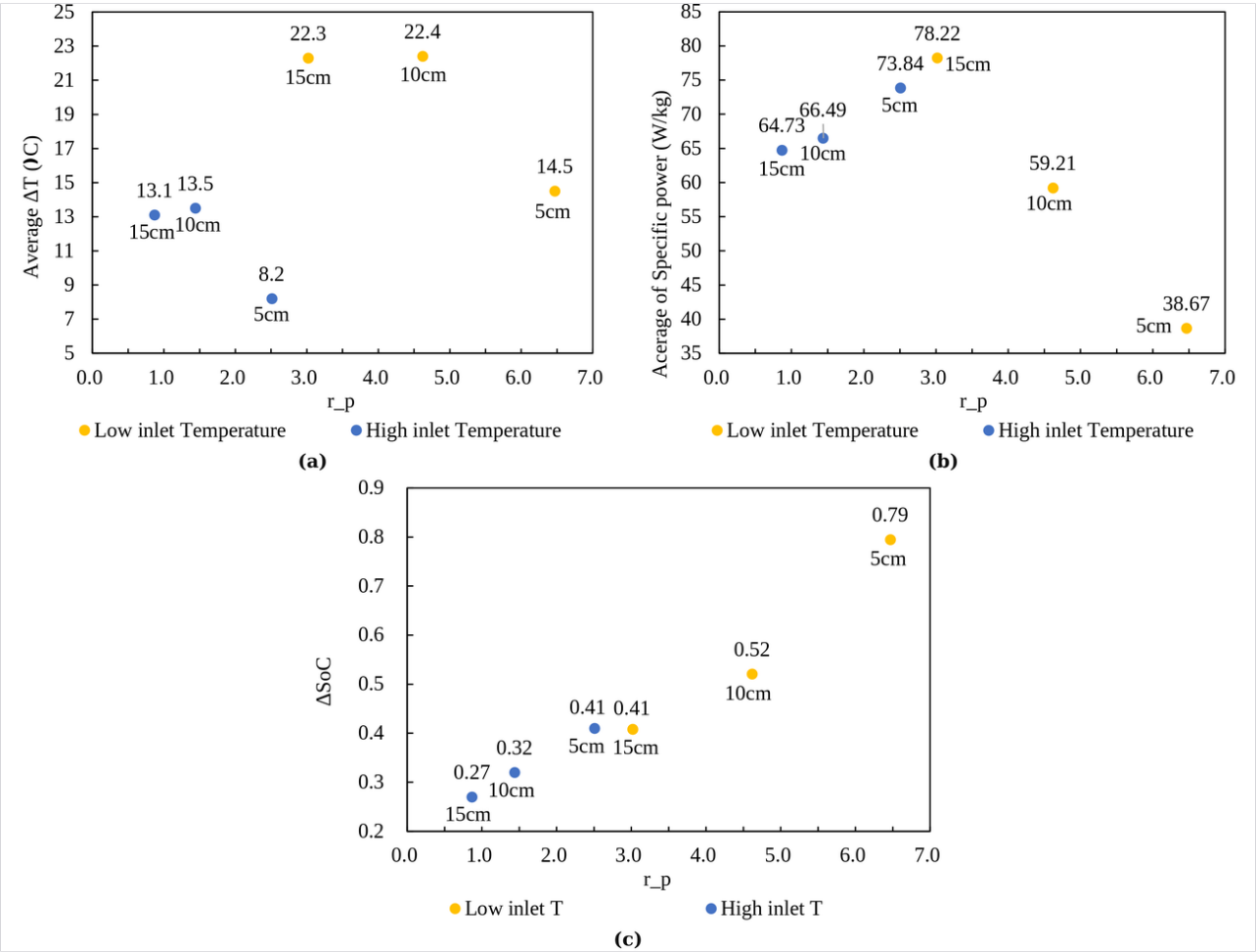

Figure 3. Relationships between r_p and the performance indicators of the COCO reactor under low and high inlet temperature conditions: (a) average temperature difference; (b) average specific power; and (c) ΔSoC.

The low- and high-temperature experiments occupy distinct thermodynamic regimes, with the low temperature cases exhibiting r_p between approximately 3.02 and 6.47, while the high temperature cases remain concentrated between 0.87 and 2.51. This clear separation underscores that elevated inlet temperatures fundamentally alter the thermodynamic conditions experienced by the reactive material. Across both temperature regimes, the ΔSoC generally scales with r_p, rising from 3.02 to 6.47 in low temperature tests and from 0.87 to 2.51 under high temperature conditions. However, because r_p and ΔSoC both increase concurrently with TCM bed thickness, this positive correlation cannot be interpreted as an independent causal effect of r_p alone. A thicker bed contained more reactive material and therefore had a greater total adsorption capacity. It also changed the thermal response and material temperature of the bed, which affected the equilibrium vapour pressure used to calculate r_p. The increase in ΔSoC therefore resulted from the combined effects of adsorption conditions and bed configuration.

Ultimately, these findings suggest that r_p serves as an effective thermodynamic descriptor for the achievable extent of material hydration rather than a direct predictor of kinetic thermal output. The absence of a straightforward relationship between r_p and specific power confirms that transport related factors heavily modulate the heat release rate. This operational dependency motivates the subsequent analysis of τ and water vapor availability.

3.3. Coupled effects of characteristic residence time and inlet absolute humidity

To distinguish the effect of water vapour availability from that of air–material contact conditions, tests with comparable characteristic residence times were first compared at inlet absolute humidities of approximately 6 and 12 $g_w \cdot kg_{da}^{-1}$. Tests conducted at the same humidity but with different airflow velocities and bed thicknesses were then examined to assess the transport related effects represented by τ. The resulting relationships between τ and reactor performance are shown in Figure 4.

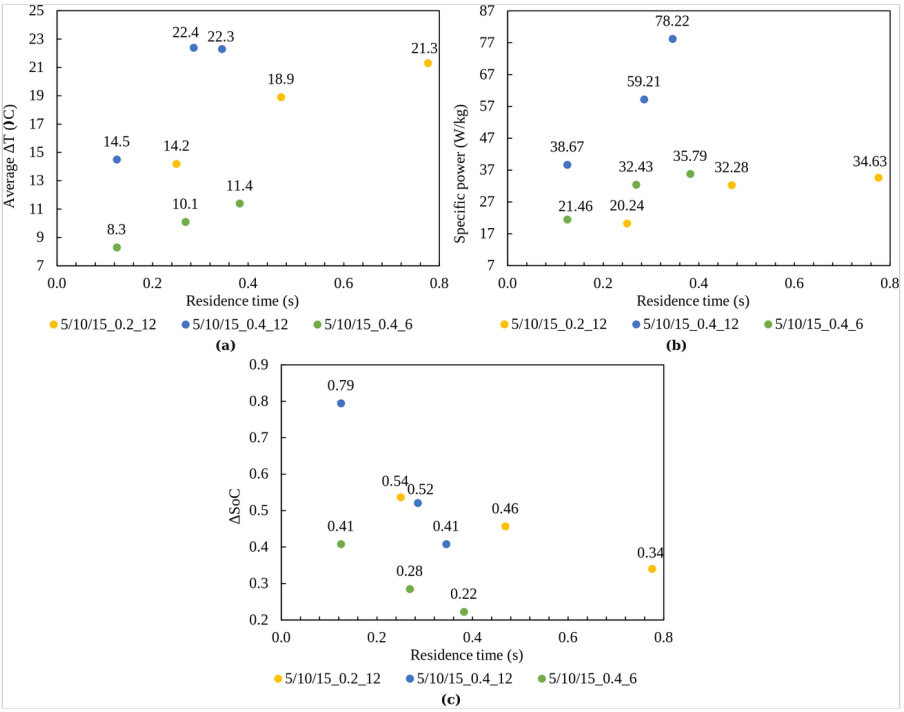

Figure 4. Relationships between characteristic residence time and the performance indicators of the COCO reactor under different airflow velocities and inlet absolute humidities: (a) average temperature difference; (b) average specific power; and (c) ΔSoC.

At comparable τ and identical airflow velocities, elevating the inlet absolute humidity from approximately 6 to 12 $g_w \cdot kg_{da}^{-1}$ substantially enhances the average ΔT. For instance, at a residence time of 0.28–0.30 s, the average ΔT climbs from roughly 10 °C under low humidity to 22 °C under high humidity. A parallel trend is observed for the average specific power, which exhibits up to a twofold increase under high humidity conditions. These results indicate that heightened water vapor availability intensifies both the thermal response magnitude and the heat release rate, demonstrating that τ alone is insufficient to fully dictate reactor performance.

Conversely, under uniform absolute humidity, configurations with shorter residence times driven by higher airflow velocities-generally yield greater average specific power. Interestingly, the average ΔT does not follow this trend; similar ΔT values are sustained across disparate residence times, even when the corresponding specific power varies substantially. This divergence underscores that ΔT and specific power capture fundamentally different facets of reactor behaviour. While longer residence times can maintain a high temperature differential, elevated airflow rates accelerate both heat extraction and water vapor delivery, thereby maximizing specific power. Thus, the enhanced power output at shorter residence times is not a direct consequence of reduced contact time, but rather a reflection of concurrent transport enhancements: increased air mass flow rate, accelerated vapor supply, and intensified convective heat and mass transfer.

Regarding material utilization, the ΔSoC generally decreases as τ increases, with the peak ΔSoC achieved under the combined conditions of high absolute humidity and high airflow velocity. Conversely, restricted vapor availability severely limits the final extent of material hydration. This

downward trend in ΔSoC with increasing τ, however, cannot be isolated as an independent effect of residence time. Because variations in τ inherently involve concurrent adjustments to both bed thickness and flow conditions, material utilization over a fixed operational period must instead be understood as a coupled function of vapor availability, mass delivery rates, air flow velocity, physical bed configuration, and internal transport resistance. Ultimately, τ serves as a transport descriptor rather than an independent governing parameter. While a longer residence time theoretically provides greater opportunity for local fluid-solid exchange, it simultaneously implies either thicker beds, which introduce extended internal transport paths, or lower airflow velocities that restrict vapor supply and thermal extraction. Consequently, residence time must be integrated with mass flow and boundary conditions to comprehensively map reactor performance.

4. Conclusion

This study further examined the effect of elevated inlet temperature on the discharge behaviour of an open-loop TCES reactor filled with a vermiculite-$CaCl_2$ composite. The existing experimental dataset was reinterpreted from thermodynamic and transport related perspectives using r_p and τ. The results showed that increasing the inlet temperature from 18 °C to 43–50 °C reduced the pressure ratio from approximately 3.02–6.47 to 0.87–2.51 and limited the cumulative specific energy to about 60–70 $Wh \cdot kg^{-1}$. Bed thickness still affected the temperature rise, but the 5 cm bed achieved the highest specific energy per unit mass, indicating lower material utilisation in thicker beds.

Water vapour availability and airflow mainly controlled the rate of heat release. At comparable characteristic residence times, increasing the inlet absolute humidity from approximately 6 to 12 $g_w \cdot kg_{da}^{-1}$ produced up to a twofold increase in average specific power. Higher airflow also increased vapour delivery and heat extraction, although it reduced the τ. These findings showed that r_p and τ should be interpreted together, as reactor performance could not be explained by a single operating parameter.

A preliminary empirical relationship was also developed from the experimental dataset to describe transient discharge power as a function of time and the main operating variables. The current fitting indicated that inlet temperature and airflow velocity had the strongest effects on peak power and discharge curve shape, while humidity mainly affected hydration progress and response time. Bed thickness showed a smaller direct effect but remained relevant through its interaction with airflow and internal transport. The fitted coefficients were used to estimate the contribution of each factor and their interactions. The complete formulation and contribution ratios will be reported after further validation.

Declarations

Author contributions. Zhuo Chang: Conceptualization, Methodology, Writing (original draft), Data curation, Formal analysis, Investigation, Visualization, Validation, Resources. Eleonora Baccega: Conceptualization, Methodology, Writing (review and editing), Validation, Supervision, Software. Moussa Aidi: Methodology, Data curation, Formal analysis, Software. Michele Bottarelli: Conceptualization, Writing (review and editing), Supervision, Validation, Project administration, Resources, Funding acquisition.

Funding. This research received support from the ECHO project (Efficient Compact modular tHermal energy storage system), funded by the European Union's Horizon Europe research and innovation programme under Grant Agreement No. 101096368, and the SACER project (Sviluppo e integrazione di Accumuli innovativi nelle Comunità Energetiche Rinnovabili), funded by the ERDF programme of the Emilia-Romagna Region, Italy, under Grant Agreement No. J47G22000760003.

Awards. European Commission (101096368); and Regione Emilia-Romagna (J47G22000760003)

Conflicts of interest. The authors declare no competing interests.

Data availability. The data that support the findings of this study are available from the corresponding author upon reasonable request.

Ethics. Not applicable. This study did not involve human participants or animals and did not require ethical approval.

Generative AI. During the preparation of this manuscript, the authors used ChatGPT (OpenAI) to assist with language refinement, text organization, and improving the clarity of the manuscript. All scientific content, data analysis, and conclusions were reviewed and verified by the authors, who take full responsibility for the final published work.

Acknowledgements. The authors gratefully acknowledge the support of the ECHO project (Efficient Compact modular Thermal energy storage system), funded by the European Union's Horizon Europe research and innovation programme under Grant Agreement No. 101096368. Additional support was provided by the SACER project (Sviluppo e integrazione di Accumuli innovativi nelle Comunità Energetiche Rinnovabili), funded by the ERDF programme of the Emilia-Romagna Region (Italy) under grant agreement No. J47G22000760003.

References

Aristov, Yu.I.; Restuccia, G.; Tokarev, M.M.; Buerger, H.-D.; Freni, A. (2000) 'Selective Water Sorbents for Multiple Applications. 11. $CaCl_2$ Confined to Expanded Vermiculite', *Reaction Kinetics and Catalysis Letters*, 71(2), pp. 377-384. Available at: https://doi.org/10.1023/a:1010351815698

Aydin, Devrim; Casey, Sean P.; Chen, Xiangjie; Riffat, Saffa (2016) 'Novel "open-sorption pipe" reactor for solar thermal energy storage', *Energy Conversion and Management*, 121, pp. 321-334. Available at: https://doi.org/10.1016/j.enconman.2016.05.045

Baccega, E; Zhang, Y; Su, Y; Bottarelli, M (2025) 'Development of a numerical model of $CaCl_2$ hydration and dehydration reaction for thermochemical energy storage', *Journal of Physics: Conference Series*, 2940(1), pp. 012027. Available at: https://doi.org/10.1088/1742-6596/2940/1/012027

Baghapour, Behzad; Rouhani, Mina; Sharafian, Amir; Kalhori, Sahand Behboodi; Bahrami, Majid (2018) 'A pressure drop study for packed bed adsorption thermal energy storage', *Applied Thermal Engineering*, 138, pp. 731-739. Available at: https://doi.org/10.1016/j.applthermaleng.2018.03.098

Chen, Jianbin; Zhang, Yong; Chen, Ziwei; Gan, Guohui; Su, Yuehong (2025) 'Impact of porous host materials on the compromise of thermochemical energy storage performance', *Renewable Energy*, 245, pp. 122784. Available at: https://doi.org/10.1016/j.renene.2025.122784

Chen, Jianbin; Chen, Ziwei; Keskin, Ismail Kaan; Zhang, Yong; Su, Yuehong (2026) 'A study on correlation between volumetric salt content and hydration kinetics of vermiculite-$CaCl_2$ composites via variable preparation methods', *Energy Conversion and Management*, 353, pp. 121230. Available at: https://doi.org/10.1016/j.enconman.2026.121230

Enasel, Eduard; Dumitrascu, Gheorghe (2025) 'Storage solutions for renewable energy: A review', *Energy Nexus*, 17, pp. 100391. Available at: https://doi.org/10.1016/j.nexus.2025.100391

Gaeini, M.; Wind, R.; Donkers, P.A.J.; Zondag, H.A.; Rindt, C.C.M. (2017) 'Development of a validated 2D model for flow, moisture and heat transport in a packed bed reactor using MRI experiment and a lab-scale reactor setup', *International Journal of Heat and Mass Transfer*, 113, pp. 1116-1129. Available at: https://doi.org/10.1016/j.ijheatmasstransfer.2017.06.034

Gaeini, M.; Rouws, A.L.; Salari, J.W.O.; Zondag, H.A.; Rindt, C.C.M. (2018) 'Characterization of microencapsulated and impregnated porous host materials based on calcium chloride for thermochemical energy storage', *Applied Energy*, 212, pp. 1165-1177. Available at: https://doi.org/10.1016/j.apenergy.2017.12.131

Gao, Shichao; Wang, Shugang; Hu, Peiyu; Wang, Jihong (2025) 'Prediction method of adsorption thermal energy storage reactor performances based on reaction wave model', *Applied Energy*, 377, pp. 124363. Available at: https://doi.org/10.1016/j.apenergy.2024.124363

Hosouli, S.; Sutton, R.J.; Searle, J.; Jewell, E.; Elvins, J. (2026) 'Importance of reactor design on efficient utilisation of thermochemical heat storage materials for background space heating', *Journal of Energy Storage*, 142, pp. 119509. Available at: https://doi.org/10.1016/j.est.2025.119509

Kieskamp, B.; Mahmoudi, A.; Shahi, M. (2024) 'A novel multi-reactor system for thermochemical heat storage through detailed modeling of K_2CO_3 particles', *Journal of Energy Storage*, 78, pp. 110028. Available at: https://doi.org/10.1016/j.est.2023.110028

Kinzer, Bryan; Ghosh, Durga Prasad; Crowley, Declan; Jatkar, Arijit; Bala Chandran, Rohini (2025) 'Impact of scaling and design on salt hydrate thermochemical energy storage performance', *Applied Thermal Engineering*, 272, pp. 126160. Available at: https://doi.org/10.1016/j.applthermaleng.2025.126160

Sullivan, Geraint; Griffiths, Chris; Jewell, Eifion; Searle, Justin; Elvins, Jonathon (2023) 'Cycling Stability of Calcium-Impregnated Vermiculite in Open Reactor Used as a Thermochemical Storage Material', *Energies*, 16(21), pp. 7225. Available at: https://doi.org/10.3390/en16217225

Suraparaju, Subbarama Kousik; Samykano, Mahendran; Vennapusa, Jagadeeswara Reddy; Rajamony, Reji Kumar; Balasubramanian, Dhinesh; Said, Zafar; Pandey, Adarsh Kumar (2025) 'Challenges and prospectives of energy storage integration in renewable energy systems for net zero transition', *Journal of Energy Storage*, 125, pp. 116923. Available at: https://doi.org/10.1016/j.est.2025.116923

Valverde, Abel; Cabrera-Codony, Alba; Calvo-Schwarzwalder, Marc; Myers, Timothy G. (2024) 'Investigating the impact of adsorbent particle size on column adsorption kinetics through a mathematical model', *International Journal of Heat and Mass Transfer*, 218, pp. 124724. Available at: https://doi.org/10.1016/j.ijheatmasstransfer.2023.124724

Zeng, Yi; Clark, Ruby-Jean; Galazutdinova, Yana; Odukomaiya, Adewale; Al-Hallaj, Said; Farid, Mohammed; Kaur, Sumanjeet; Woods, Jason (2024) 'Open-cycle thermochemical energy storage for building space heating: Practical system configurations and effective energy density', *Applied Energy*, 376, pp. 124218. Available at: https://doi.org/10.1016/j.apenergy.2024.124218

Zhang, Yong; Chen, Ziwei; Zhang, Yanan; Su, Yuehong; Riffat, Saffa (2024) 'Parameter control in synthesis of Vermiculite-$CaCl_2$ composite materials for thermochemical adsorption heat storage', *Energy*, 291, pp. 130478. Available at: https://doi.org/10.1016/j.energy.2024.130478

HOW TO CITE THIS PAPER

Chang, Z., Baccega, E., Aidi, M. and Bottarelli, M. (2026). Coupled Effects of Thermodynamic Conditions, Bed Configuration and Airflow Characteristics on the Performance of an Open-Loop Thermochemical Energy Storage Reactor. In: *Proceedings of the 22nd International Conference on Sustainable Energy Technologies (SET2026)*, Kuala Lumpur, Malaysia, 13 to 15 August 2026. Caravel Press, pp. 109–120. ISBN 978-1-995850-00-9. ISSN 2978-4387. https://doi.org/10.65582/set.2026.009

COPYRIGHT AND LICENCE

© 2026 The Author(s). This is an open access paper distributed under the terms of the Creative Commons Attribution (CC BY 4.0) licence, which permits unrestricted use, distribution and reproduction in any medium, provided the original work is properly cited.

WSSET World Society of Sustainable Energy Technologies Organised by the World Society of Sustainable Energy Technologies. Published by Caravel Press.